

# LUMINESCENCE IMAGING FOR FAST SHUNT LOCALIZATION IN SILICON SOLAR CELLS AND SILICON WAFERS

T. Trupke, R.A. Bardos, M.D. Abbott and K. Fisher  
Centre of Excellence for Advanced Silicon Photovoltaics and Photonics,  
University of New South Wales, Sydney, NSW, 2052, Australia, thorsten@trupke.de

J. Bauer and O. Breitenstein  
Max Planck Institute for Microstructure Physics, 06120 Halle, Germany

**ABSTRACT:** Photoluminescence and electroluminescence imaging are demonstrated as fast characterization tools to identify shunt locations in both fully and partially processed silicon solar cells. The spatial shunt distribution obtained from luminescence images taken on industrial screen printed silicon solar cells is found to agree with a quantitative lock-in thermography shunt analysis. The short data acquisition times of typically one second per wafer suggest potential applications of luminescence imaging for in-line shunt localization in industrial solar cell manufacturing. Various potential applications of luminescence imaging to reduce the negative impact of shunts on the average yield and efficiency in industrial manufacturing are suggested and discussed.

## 1 INTRODUCTION

The shunt resistance  $R_{SH}$  (also referred to as parallel resistance) is a crucial electrical parameter that affects the open circuit voltage and the fill factor and thereby the efficiency of solar cells. In silicon solar cells the lumped (i.e. spatially averaged) shunt resistance is often dominated by highly localized shunts, i.e. by local short circuits of the pn-junction. An example for material induced shunts are conductive channels formed by SiC precipitates in block cast silicon [1,2]. Processing induced shunts can be caused for example by non-ideal firing or plating conditions if the metal forms a conductive path between a p-type and an n-type region of the junction. When highly defective and thus recombination active regions cross the junction as for example at the edge of screen printed solar cells, the enhanced local recombination in combination with the limited conductivity of the emitter can also cause a shunt like IV characteristics [3]. Edge isolation techniques are therefore used in industrial manufacturing to avoid the influence of shunts on the cell efficiency (because the negative influence of local regions of strongly enhanced recombination on the terminal characteristics at the maximum power point is very similar to the impact of shunts we will refer to both mechanisms as *shunts* throughout this paper). Mitigating shunt effects around the edge of a solar cell is comparatively straightforward because likely shunt positions (i.e. entire edge region) are known. Various material or processing induced shunts are however located within the active cell area. Experimental methods to localize shunts are thus required. Some existing methods to localize shunts are based on measuring local temperature variations. Liquid crystal sheets that change their color upon temperature variations allow a very crude localization of shunts. Lock-in thermography (LIT) methods allow a very quantitative analysis of the position and the electrical parameters of even weak shunts [4]. CELLO [5] and LBIC are *mapping* techniques, that allow spatial information about local shunts to be obtained. None of those techniques is at the time of writing fast enough for in-line monitoring of each solar cell or wafer going through a modern solar cell production line.

Here we would like to demonstrate that photoluminescence (PL) and electroluminescence (EL) imaging on silicon wafers and silicon solar cells [6, 7], while not as accurate at this stage as LIT techniques in

terms of identifying quantitative electrical parameters of shunted regions, are powerful experimental methods suitable for in-line shunt localization, allowing a variety of industrially relevant applications as discussed below.

## 2 LUMINESCENCE IMAGING

EL- and PL-imaging have recently been introduced as fast and efficient characterization techniques [6, 8], providing spatial information about the minority carrier diffusion length in silicon solar cells [8], and about the minority carrier lifetime in silicon wafers [6]. It has also been shown recently that the combination of EL imaging and PL imaging, i.e. PL imaging with external bias control, is a non-destructive and very fast new method to obtain high resolution images of variations in the series resistance in finished solar cells [7].

Here, a thermoelectrically cooled silicon CCD cameras is used to capture the spatially resolved luminescence emitted by the sample. In EL imaging a forward bias is applied to finished cells in the dark in order to excite the luminescence. In PL imaging a 25 W laser is used to illuminate samples up to 12.5x12.5 cm<sup>2</sup> in size homogeneously and with up to one Sun equivalent illumination intensity.

## 3 MATERIAL INDUCED SHUNTS

Fig.1 shows an EL (top) and a PL image (bottom) taken on a 12.5x12.5 cm<sup>2</sup> industrial screen printed multicrystalline silicon solar cell, that was rejected by the manufacturer due to a low efficiency of only 9.6%. The latter is caused by the poor fill factor of 53.1%, which in turn is caused by shunts. Both images in Fig.1 were taken with the equivalent of about one Sun excitation conditions, i.e. with 30 mAcm<sup>-2</sup> forward current density in the dark (EL) and with the equivalent of 1 Sun monochromatic illumination in PL. Because a suitable probing station with multiple probes along the busbars was not available for this study, four single contact probes were used to inject the current in EL measurements. Some of the probes can be seen in the EL image in Fig.1 (top) and the influence of the series resistance of the busbar on the EL intensity distribution is also evident (brighter intensity in the vicinity of the probes). However, both images clearly indicate the locations of shunts within that cell, i.e. in the bottom half of the central region between the busbars. Compared to

the recombination-active grain boundaries, which are also visible in these images, the shunts are characterized by a blurred circular appearance.

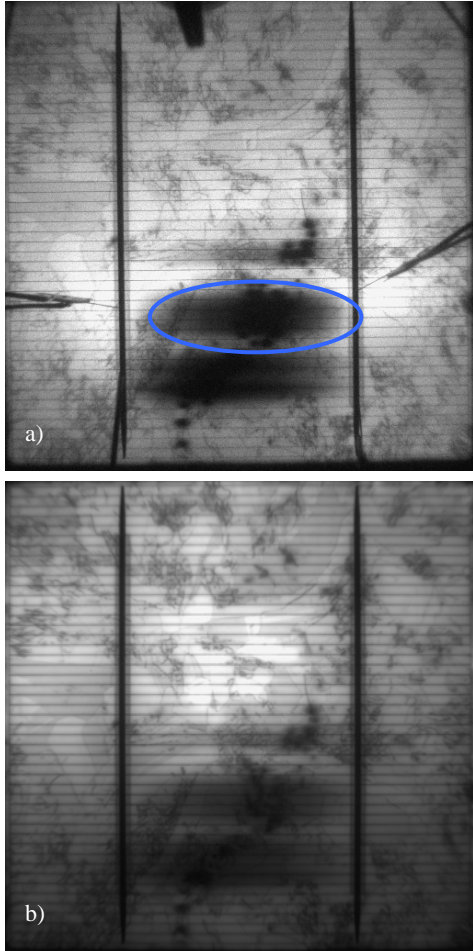


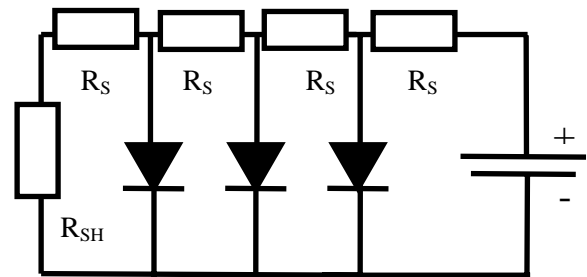
**Figure 1:** Electroluminescence image (a) and photoluminescence image (b) of a 12.5x12.5 cm<sup>2</sup> screen printed silicon solar cell

The contrast in both images around the shunted areas is a series resistance effect caused by the limited conductivity of the emitter. To elucidate this point Fig.2 shows a simplified equivalent circuit in which diodes, representing different lateral areas of a cell are connected in parallel through individual series resistance elements  $R_S$ , that represent the lateral resistance of the emitter. The shunted region is represented by a resistor  $R_{SH}$  that is connected to the diodes in parallel. That resistor could be replaced by a diode with very large dark saturation current in order to represent a high recombination area rather than a shunt.

The shunted regions locally draw a much higher current density than the emitter and the contact-grid in a typical solar cell are designed for. As a result substantial voltage drops occur over the series resistance elements in the vicinity of the shunt, leading to an increasing reduction in the voltage across each diode element with decreasing distance to the shunted area. If we imagine the diodes in Fig.2 to represent equidistant circular elements then it is easily seen how the series resistance of the emitter results in the circular shaped areas of reduced luminescence intensity around the shunts that are observed in Fig.1. LBIC measurements with similar circular shaped areas of reduced current collection

efficiency around local shunts have been reported and explained by equivalent series resistance effects [9].

The positions of some shunts (e.g. area marked with blue line in Fig.1a) appear blurred in the luminescence images, an effect caused either because these shunts are in direct contact or in very close proximity to the metal lines or because a large number of local shunts is located in the same area. In those areas the shunts draw enough current that the same series resistance effects that were discussed above for the emitter sheet resistance now also occur within the metal fingers that supply the current to those areas. Variation of the contrast of these images, variation of the excitation conditions (current density in EL, illumination intensity in PL) are various options to get better spatial information about the shunts in those regions. PL measurement prior to the metallization is an obvious method to avoid this smearing effect caused by the metal lines.



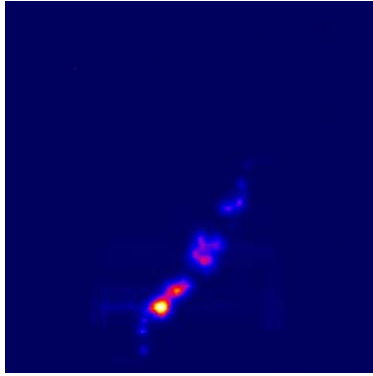
**Figure 2:** Equivalent circuit of a shunted solar cell with lateral variations of the material quality.

Fig.3 shows a dark LIT measurement taken on the same cell under 0.5V forward bias conditions that shows localized shunts in the central area of the cell. Comparison of LIT measurements under forward and under reverse bias at 0.5V revealed an ohmic nature of those shunts. High resolution LIT images show that the shunted regions are caused by a variety of small point like spots with dimensions on the order of a few micrometers only, which indicates that these shunts are caused by highly conductive SiC filaments intersecting the junction. Comparison with the luminescence images from Fig.1 shows good lateral correlation between the shunted areas identified with the two techniques. This clearly shows that luminescence imaging is suitable for shunt localization in industrial silicon solar cells.

Both images in Fig.1 were taken with an exposure time of only one second each, demonstrating that in-line shunt localization on each cell in industrial solar cell manufacturing is feasible.

#### 4 PROCESSING INDUCED SHUNTS

Various sources of *processing induced* shunts exist in both industrial manufacturing and in a research environment, e.g. during the development of new device concepts and related process optimization. Some examples of processing induced shunts that were monitored with luminescence imaging by the buried contact solar cell group at UNSW during device developments will now be discussed. During the development of improved buried contact solar cell designs various 225  $\mu\text{m}$  thick 1  $\Omega\text{cm}$  n-type float zone wafers first received a boron emitter diffusion. Base



**Figure 3:** Dark lock-in thermography image of the cell from Fig.1 taken with 0.5 V forward bias.

contacts were established by a laser process to cut contact grooves through the emitter followed by a phosphorous groove diffusion, nickel plating and nickel sintering. During process optimization this sequence is particularly prone to processing induced shunts. Shunts are likely to occur wherever nickel is inadvertently deposited on the surface during plating, e.g. in areas where the surface is damaged. The subsequent sintering process is likely to fire the deposited nickel through the emitter into the base, thereby causing a shunt. In addition shunts are also expected in the grooves in localized areas where the phosphorous groove diffusion does not compensate the emitter diffusion at the intersection of the groove with the emitter [10]. Metal deposition in the groove and subsequent sintering will then unavoidably lead to a shunt.

PL images were taken on various samples after groove diffusion, after nickel deposition and after nickel sintering. In addition quasi steady state photoluminescence (QSS-PL) lifetime measurements and implied IV curves from Suns-PL were measured after each of those steps. The images provide spatial information (i.e. about the position of shunts) while the QSS-PL lifetime [11] and Suns-PL [12] measurements give quantitative information about the impact of those shunts on the terminal characteristics. Fig.4 shows an example of this characterization sequence. The one-Sun PL images show how the nickel sintering step (bottom left) leads to a strong shunt in the middle of the cell and various smaller shunts (blue circles). The lifetime curves (top left) and the implied IV curves (top right) show the quantitative influence of those shunts and of each processing step on the terminal characteristics.

The bottom right image in Fig.4 is also taken after nickel sintering but with much lower,  $\sim 0.1$  Sun equivalent illumination. That image is an example of how at low current densities, local shunts or areas of locally enhanced recombination have an impact on the device properties over a much larger area in the presence of an emitter. At lower current densities the emitter connects larger lateral regions of the cell in parallel. The base contact laser grooves form trenches in the emitter, which explains why the negative impact of the local shunt is only affecting the carrier density in the region between two grooves, leading to the rectangular regions of reduced luminescence. In contrast, at higher intensities (bottom left) the limited conductivity of the emitter effectively isolates local shunts or recombination active regions from high lifetime regions that are located at a

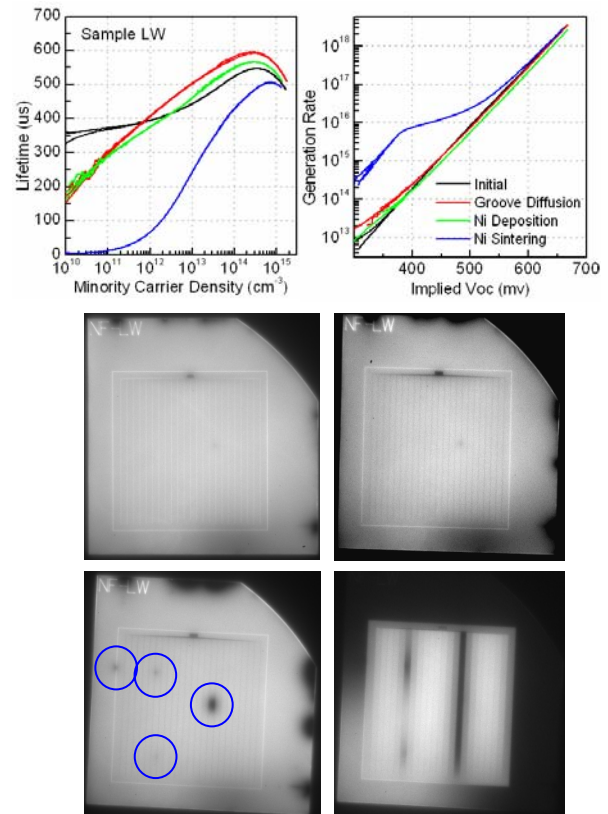


**Figure 4:** One Sun PL images of a 1  $\Omega$ cm n-type wafer after emitter formation, laser grooving and heavy groove diffusion, (middle left), subsequent nickel deposition (middle right), subsequent nickel sintering (bottom left) and 0.1 Sun PL image after nickel sintering (bottom right). Top left: Corresponding injection level dependent QSS-PL lifetime curves, top right: corresponding implied IV curves from Suns-PL

sufficient distance.

In the example shown in Fig.4 a heavy groove diffusion was used for the base contact. Fig.5 shows a one-Sun PL image of a wafer after nickel sintering, with a lighter phosphorous groove diffusion and otherwise identical processing. Clearly there are a much larger number of shunts visible in that case which is explained by the fact that the lighter phosphorous diffusion cannot sufficiently compensate the emitter diffusion at the intersection with the groove, leading to a higher density of shunted regions. These examples show how the combination of PL imaging with QSS-PL measurements allows a very efficient and accurate optimization of the processing conditions and the elimination of shunts.

## 5 IN-LINE APPLICATIONS

Shunting is a common problem in cell manufacturing, a problem that is likely to become worse with the requirement to use cheaper and more defect-rich wafers. The short data acquisition times (on the order of one second per measurement) typically required for high resolution luminescence images allow various applications, that will be discussed below. These could lead to a significantly reduced impact of shunting on average cell production yield and efficiency in industrial cell manufacturing.

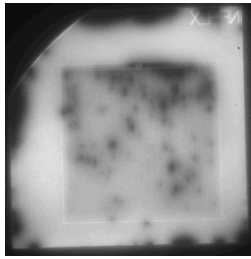


**Figure 5:** One Sun PL image of a wafer with lighter phosphorus groove diffusion (compared to the sample from Fig.4), resulting in a higher density of local shunts.

### 5.1 Finished cells

The examples shown in this paper demonstrate that EL or PL images taken on fully processed silicon solar cells allow an accurate localization of shunted areas. On the other hand, laser edge isolation methods to eliminate shunts from the edge region of industrial screen printed cells are already applied in industrial production. This suggests that if the location of a shunt is known, similar laser isolation methods, e.g. by cutting a circular trench into the emitter and, if necessary through metal lines around the shunted areas, could be applied to reduce or eliminate the impact of those shunts on cell performance.

It is clear that shunted cells with efficiencies dramatically below average cell efficiencies represent a substantial financial loss to cell manufacturers, which suggests that comparatively small additional experimental effort to recover the efficiency of those cells may be economically warranted. Sorting shunted cells into bins is straightforward in a modern production environment. A specialized shunt isolation line that identifies the shunts in all cells from the “shunted-bin” and subsequently electrically isolates the shunts in those cells only requires a luminescence imaging set up, a precision laser system and either image processing software or manual intervention to feed the information obtained from the luminescence image back to the laser system. For multicrystalline cells, a challenge will be to automatically distinguish shunts from other recombination active defects. Because the fraction of shunted cells is typically on the order of only a few percent of total throughput, existing edge isolation lasers could actually be used for that task during downtimes of the production line, hence avoiding the requirement of a separate laser system. Alternatively the shunted cells from say ten separate production lines could be collectively recovered to acceptable efficiencies with a specialized shunt isolation line.

As an alternative, luminescence imaging of every cell could be integrated into the production line prior to the laser edge isolation step and isolation circles would be written around internal shunts in addition to the edge isolation trench. In that case, advantageously each cell would be monitored with luminescence imaging, which allows information to be obtained not only about shunts but also about locally enhanced series resistance, contamination problems, handling problems, cracks, etc.

### 5.2 Partially processed cells

As a contactless technique, PL imaging can be applied to silicon wafers at any processing stage. Material induced shunts already show up in PL images after the emitter diffusion. This allows those wafers to be removed from the line that are likely to result in a shunted cell. Alternatively, the laser isolation methods discussed above could be applied immediately after

emitter formation. In this case the laser edge isolation should also be carried out immediately after the emitter formation, which would have the further advantage that isolation trenches through the emitter would subsequently be passivated during SiN deposition and firing. In addition, the knowledge of the position of localized shunts after emitter formation could be used to optimize (e.g. by image processing algorithms) the position of the front surface grid to minimize direct contact between shunted areas and the metal lines. The same idea can be applied to advanced cell concepts such as screen printed solar cells with semiconductor fingers [13], where the laser processes to scribe the fingers could be guided to avoid shunted regions.

## 6 CONCLUSIONS

The fast localization of shunts in silicon wafers and solar cells by luminescence (PL and EL) imaging has been demonstrated. Though this technique is not as sensitive to weak shunts and at this stage not as quantitatively interpretable as lock-in thermography, its unsurpassed speed of 1s per measurement makes it very attractive for in-line shunt monitoring in production. Various methods to reduce the negative impact of shunts on average efficiency and yield in industrial manufacturing were discussed. Combined with a variety of other appealing aspects of luminescence imaging that have recently been discovered, we believe that inline monitoring of silicon wafers and solar cells with luminescence imaging, possibly after various individual processing steps, should be part of every modern production line in the not too distant future.

**Acknowledgement** The Centre of Excellence for Advanced Silicon Photovoltaics and Photonics is funded by the Australian Research Council. The authors thank Holger Neuhaus, Deutsche Cell, for providing screen printed industrial solar cells investigated in this study.

## REFERENCES

1. M.H.A. Rifai, O. Breitenstein, J.P. Rakotoniaina, et al., 19th EPVSC, Paris (2004) 632.
2. J.P. Rakotoniaina, O. Breitenstein, M. Werner, et al., 20th EPVSC, Barcelona (2005).
3. K.R. McIntosh, PhD thesis, UNSW, Sydney (2001).
4. O. Breitenstein, M. Langenkamp, J.P. Rakotoniaina, et al., 17th EPVSC, Munich (2001) 1499-1502.
5. J. Carstensen, G. Popkirov, J. Bahr, et al., *Solar Energy Materials and Solar Cells* **76** (2003) 599.
6. T. Trupke, R.A. Bardos, M.C. Schubert, et al., *Applied Physics Letters* **89** (2006) 044107.
7. T. Trupke, R.A. Bardos, M.D. Abbott, et al., WCPEC-4, Waikoloa, USA (2006).
8. T. Fuyuki, H. Kondo, T. Yamazaki, et al., *Applied Physics Letters* **86**(26) (2005) 262108.
9. A. Kaminski, O. Breitenstein, J.P. Boyeaux, et al., *Journal of Physics: Condensed Matter* **16** (2004) S9.
10. J.H. Guo, PhD thesis, UNSW, (2004).
11. T. Trupke and R.A. Bardos, 31st IEEE PVSC, Orlando, USA (2005).
12. T. Trupke, R.A. Bardos, M.D. Abbott, et al., *Applied Physics Letters* **87** (2005) 093503.
13. S.R. Wenham, L. Mai, B. Tjahjono, et al., 15th PVSEC, Shanghai, China (2005).